Partially Bound Systems as Sensitive Probes of Microsolvation: A Microwave and ab Initio Study of HCN···HCN−BF_3

D. L. Fiacco[†] and K. R. Leopold*

Department of Chemistry, University of Minnesota, 207 Pleasant Street South East, Minneapolis, Minnesota 55455

Received: October 17, 2002; In Final Form: January 31, 2003

The complex HCN···HCN−BF_3 has been investigated by rotational spectroscopy and ab initio methods. The experimental B−N bond distance is 2.299(28) Å, which represents a contraction of 0.174(57) Å relative to that previously determined in HCN−BF_3. The observed N···H distance, on the other hand, is 2.185(25) Å, which is only 0.045(25) Å shorter than that in $(HCN)_2$. A block-localized wave function energy decomposition analysis indicates that significant energetic differences between HCN−BF_3 and HCN···HCN−BF_3 arise from a combination of distortion, polarization, and charge-transfer energies, with the net result that the remote HCN unit increases the effective dative bond energy by about 20%. In addition, electron density difference maps reveal migration of charge from the inner nitrogen to the boron atom. The large magnitude of the bond contraction, the increase in bond strength, and the flow of charge from HCN to BF_3 indicate that the additional HCN unit drives the dative bond formation forward within the HCN−BF_3 complex. The effect is large, even at a very small degree of microsolvation, demonstrating an intrinsic hypersensitivity to near neighbor interactions which we attribute to the partially bonded character of HCN−BF_3. We suggest that partially bound complexes, in general, are highly sensitive probes of their local environment and may represent an interesting class of systems in which to investigate microsolvation effects.

Introduction

Understanding the influence of solvent on molecular energetics and reactivity is an important goal in chemistry.[1−3] Among the various models which have been created to calculate the thermodynamic, kinetic, and spectroscopic properties of solutions,[4] methods involving continuum representations of the solvent are attractive, in that they provide simple, yet successful descriptions of many solvation phenomena. An increasing number of studies, however, employing both continuum models as well as molecular dynamics and Monte Carlo techniques, now explicitly include some number of solvent particles in the immediate vicinity of the solute, and in doing so offer more realistic treatments of first-solvent-shell interactions.[5] Indeed, the most detailed understanding of solution-phase phenomena is afforded by a full and accurate knowledge of individual solute−solvent interactions, and for this reason, the study of small "microsolvated" clusters has also become a popular and fruitful area of investigation.[6]

Our interests over the past decade have involved the structural chemistry of Lewis acid−base complexes with partially formed dative bonds.[7,8] Such systems are unusual in that they undergo dramatic changes in structure and bonding upon crystallization and, in doing so, reveal an intrinsic hypersensitivity to near neighbor interactions. The phenomenon has been explored primarily in the context of observed gas-to-solid structure changes, but there is also strong theoretical evidence to suggest that such effects are not restricted to the highly ordered environment of a molecular crystal. Continuum models of a surrounding medium, for example, predict sizable changes in structure even at modest dielectric constants,[9,10] and a variety of theoretical studies on small, homogeneous clusters indicate significant changes during the early phases of aggregation.[11−13] Thus, it is a small step to infer that large changes in structure and bonding of partially bonded systems will also be observed in small, heterogeneous clusters as well as in bulk phase solution.

In this context, we recently reported a study of the complex HCN···HCN−SO_3, which represents the microsolvation of the partially bonded adduct HCN−SO_3 by an additional HCN "solvent" molecule.[14] We observed that while the HCN···HCN interaction in this system was essentially identical to that in $(HCN)_2$, the S−N dative bond was contracted by 0.107(21) Å relative to that in bare HCN−SO_3. Thus, a dramatic change at the dative bonding site is seen with even a single HCN neighbor, confirming the notion that partially bound systems can display large microsolvation effects, even at the very small cluster level.

Bulk phase reactions between nitriles and SO_3 produce organic, nitrogen heterocycles,[15] and thus a solid form of the HCN−SO_3 donor−acceptor adduct, to the best of our knowledge, has not been prepared. The analogous system HCN−BF_3, however, is a known compound,[16] for which both the gas phase[17] and solid state[18] molecular structures have been determined. Remarkably, the B−N bond length decreases from 2.473(29) Å in the gas-phase species to 1.638(2) Å in the solid, with a corresponding change in the geometry at the boron from nearly planar (i.e., $\sim sp^2$ hybridized boron) to nearly tetrahedral (i.e., $\sim sp^3$ hybridized boron). Moreover, while the gas phase bond length is slightly less than the sum of van der Waals radii, that in the solid is essentially the expected covalent bond distance. Thus, structural features of this system clearly indicate that the

* To whom correspondence should be addressed. E-mail: kleopold@chem.umn.edu.

[†] Present Address: Schrödinger, 120 West 45th Street, 32nd Floor, Tower 45, New York, NY 10036-4041.

10.1021/jp022245z CCC: $25.00
Published on Web 04/01/2003

partially formed B−N bond in the isolated adduct is driven to completion by the formation of the crystal.

In this work we use rotational spectroscopy of the complex HCN···HCN−BF_3 to investigate the effect of a single, dipolar "solvent" molecule on the nature of the HCN−BF_3 interaction. In addition, to further investigate aspects of the energetics and charge distribution of the system, we present a series of computational results based on the block-localized wave function energy decomposition (BLW-ED) method of Mo, Gao, and Peyerimhoff.[19] Together, the experimental and theoretical methods offer a detailed view of the effect of a single "solvent" molecule on the nature of the dative interaction, and provide further evidence for large microsolvation effects in partially bound systems. Implications for the general utility of such systems as sensitive probes of an emerging environment are also discussed.

Experimental Methods and Results

Rotational spectra of 10 isotopomers of HCN···HCN−BF_3 were obtained using the pulsed-nozzle Fourier transform microwave technique.[20] Details of the spectrometer have been given elsewhere.[21,22] The complex was produced using an injection source [23−26] in which a continuous flow of HCN (32% in argon) was introduced at a backing pressure of 125 Torr via a 0.016 in. ID stainless steel needle into the supersonic expansion several millimeters downstream from the nozzle orifice. A mixture of 2% BF_3 in Ar at a stagnation pressure of ∼1.7 atm was used to create the expansion, which was pulsed at a repetition rate of 6.5 Hz.

Isotopic substitution on the HCN was accomplished using enriched samples. DCN was prepared by reaction of KCN with dry D_3PO_4, while H^{15}N was prepared by reacting 99 atom % K^{15}N (Icon Services) with dry H_3PO_4. Due to relatively weak signals, spectra corresponding to the ^{10}B isotopomer were observed only in the case of the parent, ^{15}N/^{15}N, and fully deuterated species.

Initial spectral searches were guided using the contraction of the N−S distance in HCN···HCN−SO_3 [14] to estimate the change in the N−B bond distance relative to that in free HCN−BF_3. Spectral patterns were initially identified as belonging to HCN···HCN−BF_3 by the large number of transitions characteristic of a symmetric rotor with three quadrupolar nuclei. The process was generally straightforward, and once spectra of the parent species were located, those of most other isotopic forms were found without difficulty. Searches for the HCN···H^{15}N−BF_3 species, however, were initially unsuccessful. Returning to spectral predictions based on the geometry of the complex, it became clear that the boron-bound nitrogen is positioned almost precisely at the center of mass of the complex. While such a situation would normally give rise to a small shift to lower frequency, vibrational effects resulting from the zero-point extension of bonds are known in some cases to produce "inverted" isotope effects in which substitution by a heavier atom increases the rotational constant slightly.[27] Indeed with this in mind, searches were resumed and the transitions for the ^{15}N substituted species were quickly located, with the HC^{14}N···HC^{15}N−$^{11}BF_3$ rotational constant only a few kHz larger than that of HC^{14}N···HC^{14}N−$^{11}BF_3$.

All observed spectra displayed the characteristic patterns of a symmetric top, with quadrupolar coupling arising from various combinations of ^{10}B or ^{11}B, ^{14}N, and deuterium. A spectrum of the $J = 7 \leftarrow 6$ transition of the parent form is shown in Figure 1. Tables of observed frequencies are extensive and are provided as Supporting Information. The observed frequencies for the mono- or disubstituted H^{15}N species were readily fit to the usual symmetric rotor expression with one or two quadrupolar nuclei, as appropriate, viz.,

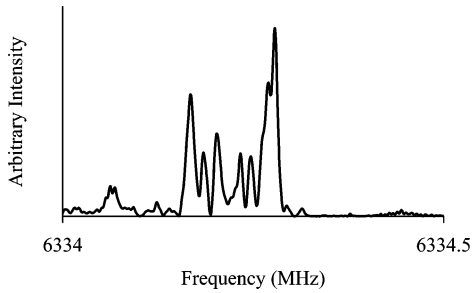

Figure 1. A portion of the $J = 7 \leftarrow 6$ transition of HC^{14}N···HC^{14}N−$^{11}BF_3$, where the splitting due to three quadrupolar nuclei is apparent. Total collection time for this spectrum was ∼47 s.

$$\nu = 2(J'' + 1)[B - D_{JK}K^2] - 4D_J(J'' + 1)^3 + \Delta E_Q \quad (1)$$

Here, ΔE_Q is the difference in hyperfine energies (in MHz) between the upper and lower states and was adequately calculated via the usual first-order treatment.[27] The other symbols have their usual meanings.[27] As is common for complexes of BF_3, many spectra showed additional, partially resolved structure due to spin−spin interactions, which was not included in the analysis. Least-squares fits of the observed spectral frequencies were carried out for isotopomers containing at least one ^{15}N nucleus, and successfully reproduced the data to within experimental uncertainties. The fitted spectroscopic constants are given in Table 1.

For species with three quadrupolar nuclei (i.e., ^{14}N and/or deuterium in both HCN units), the dense hyperfine structure, further complicated by the spin−spin interactions on the BF_3, precluded detailed assignment of individual hyperfine components. For this reason, the rotational constants were estimated from the position of the strongest transition, which is expected to correspond to that for $K = 0$ in the absence of hyperfine structure. Such an approximation is reasonably accurate, as spectral predictions (obtained from our own program as well as from that of Pickett[28]), give the strongest hyperfine component within 10 kHz of the $K = 0$ line center (in the $J = 7 \leftarrow 6$ transition). Rotational constants for the species with three coupling nuclei are also given in Table 1, where the reported uncertainties are seen to be slightly larger than those for derivatives with fully analyzed hyperfine structure.

Computational Methods and Results

To investigate aspects of energetics and charge migration upon microsolvation, calculations were performed for both HCN−BF_3 and HCN···HCN−BF_3 using the block-localized wave function energy decomposition (BLW-ED) method of Mo, Gao, and Peyerimhoff.[19] The calculations were carried out at the HF level using *Gaussian 98*,[29] though corrections to the final energy were determined at the MP2 level using the 6-31G-(2df,2pd) basis set. The energy was decomposed into five terms: ΔE_{dist}, ΔE_{es+ex}, ΔE_{pol}, ΔE_{ct}, and ΔE_{corr}. ΔE_{dist} represents the contribution to the total energy arising from the deformation of the monomer units in the complex and is always positive. ΔE_{es+ex} represents the sum of the electrostatic and exchange energies, which were not separated in the present treatment as no calculations were performed using the nonantisymmetrized wave functions necessary to explicitly evaluate the exchange contribution. ΔE_{pol} is the energy due to electronic polarization, and was calculated as the difference in energy obtained using

TABLE 1: Spectroscopic Constants for Isotopomers of HCN···HCN−BF_3[a]

isotopomer	B (MHz)	D_J (kHz)	D_{JK} (kHz)	eQq (B)	eQq (^{14}N)
$HC^{15}N-HC^{15}N-{}^{11}BF_3$	445.1364(6)	0.169(6)	4.97(1)	2.509(20)	
$HC^{14}N-HC^{15}N-{}^{11}BF_3$	452.91479(7)	0.169[b]	5.041(3)	2.509(33)	−3.984(33)
$HC^{15}N-HC^{14}N-{}^{11}BF_3$	444.6899(1)	0.170(1)	5.03(2)	2.498(13)	−3.994(22)
$HC^{15}N-HC^{15}N-{}^{10}BF_3$	447.7600(1)	0.17[b]	4.81(7)	5.047(85)	
$HC^{14}N-HC^{14}N-{}^{11}BF_3$	452.91(1)	0.17[b]			
$HC^{14}N-HC^{14}N-{}^{10}BF_3$	455.09(1)	0.17[b]			
$DC^{14}N-DC^{14}N-{}^{11}BF_3$	434.09(1)	0.17[b]			
$DC^{14}N-DC^{14}N-{}^{10}BF_3$	436.66(1)	0.17[b]			
$DC^{14}N-HC^{14}N-{}^{11}BF_3$	435.42(1)	0.17[b]			
$HC^{14}N-DC^{14}N-{}^{11}BF_3$	450.90(1)	0.17[b]			

[a] Values in parentheses are one standard error in the least-squares fit. [b] Held fixed in fit.

TABLE 2: Results of BLW-ED Calculations for HCN−BF_3 and HCN···HCN−BF_3 Using the 6-31G(2df,2pd) Basis Set[a]

	HCN−BF_3[b]	HCN···HCN−BF_3[c]	difference[d]
ΔE_{dist} (kcal/mol)	1.15	2.57	1.42
ΔE_{es+ex} (kcal/mol)	−0.77	−0.57	0.20
ΔE_{pol} (kcal/mol)	−1.89	−3.07	−1.18
ΔE_{ct} (kcal/mol)	−1.11	−2.06	−0.95
ΔE_{corr} (kcal/mol)	−1.47	−1.76	−0.29
ΔE_{tot} (kcal/mol)	−4.09	−4.89	−0.8
$\Delta\mu_{pol}$ (D)	0.804	1.101	0.297
$\Delta\mu_{ct}$ (D)	0.119	0.179	0.060
μ_{tot} (D)	4.568	9.251	4.683

[a] See text for explanation of symbols. [b] Δ refers to the difference between the HCN−BF_3 complex and the HCN and BF_3 monomers.[c] Δ refers to the difference between the HCN···HCN−BF_3 complex and HCN···HCN and BF_3 units. [d] Value for HCN···HCN−BF_3 minus the value for HCN−BF_3.

the block-localized wave function and the antisymmetrized product of the wave functions for the two monomers at the complex geometry. Similarly, the ΔE_{ct} term gives the change in energy arising from intermolecular charge transfer and was computed from the difference in energy resulting from the Hartree−Fock wave function and the block-localized wave function, correcting for basis set superposition error (BSSE).[30] Finally, ΔE_{corr} is the difference in the interaction energy between the HF and MP2 levels of theory. In the case of HCN···HCN−BF_3, the molecule was divided at the dative bond site, since our interest was in the energetic and electronic changes occurring at the B−N bond. Table 2 summarizes the results of the calculations and electron density difference maps are given for both HCN−BF_3 and HCN···HCN−BF_3 in Figure 2. Red portions of the figure represent regions of increased electron density relative to HCN and BF_3 or $(HCN)_2$ and BF_3, while the green portions represent areas of decreased electron density.

Structure Analysis of Microwave Spectra

The relevant structural parameters for HCN···HCN−BF_3 are defined in Figure 3a, and are identical to those used in our previous analysis of HCN···HCN−SO_3.[14] The possibility of large amplitude vibrational motion of the HCN and BF_3 subunits is accounted for by including the angles γ_1 and γ_2, and χ in the

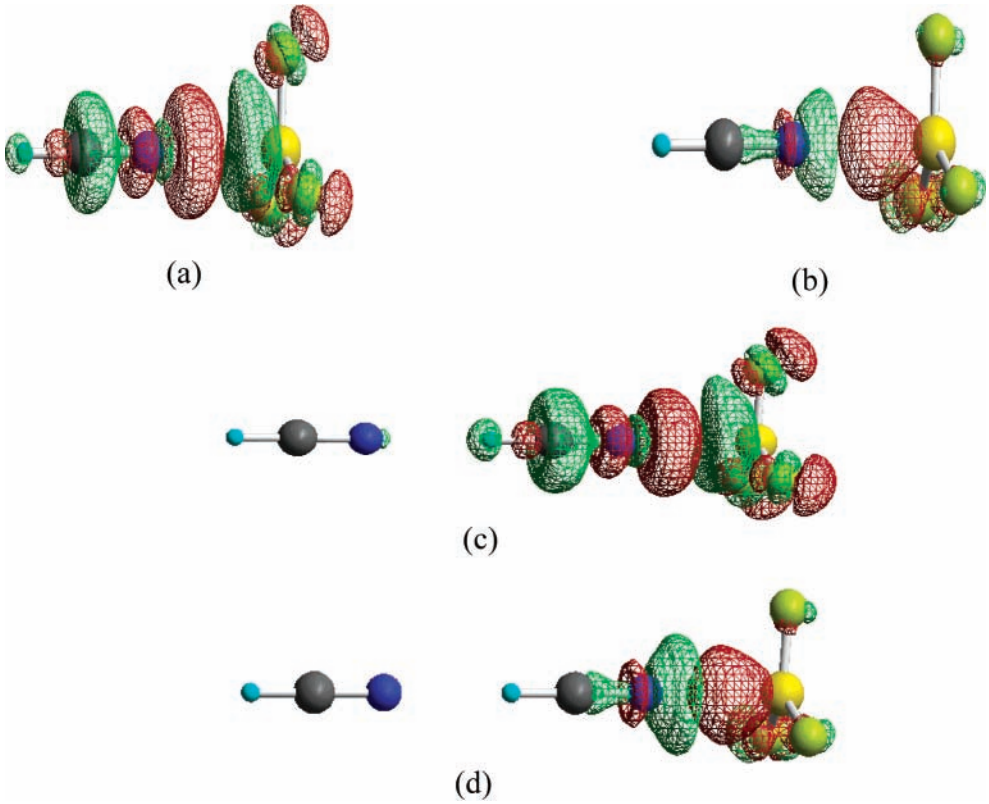

Figure 2. Electron difference density (EDD) map for HCN−BF_3 and HCN···HCN−BF_3. (a) Polarization in HCN−BF_3 (contour 0.001 e/au^3). (b) Charge-transfer in HCN−BF_3 (contour 0.0005 e/au^3). (c) Polarization in HCN···HCN−BF_3 (contour 0.001 e/au^3). (d) Charge-transfer in HCN···HCN−BF_3. (contour 0.0005 e/au^3). Red = gain of electrons. Green = loss of electrons.

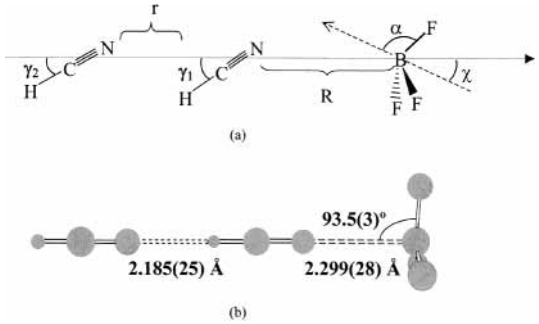

Figure 3. (a) Definition of angles used to describe the structure of HCN···HCN−BF_3. γ_1 and γ_2 give the instantaneous deviations of HCN(1) and HCN(2) from the equilibrium C_3 axis of the complex. χ is the analogous angle for the C_3 axis of the BF_3. α measures the distortion of the BF_3 unit from planarity and is equal to the NBF angle at the equilibrium geometry of the complex. *R* is the N−B distance, and *r* is the length of the HCN···HCN hydrogen bond. Angles are exaggerated in the diagram for clarity. (b) The experimentally determined vibrationally averaged structure of HCN···HCN−BF_3.

analysis. Since the complex is a symmetric top, $\langle\gamma_1\rangle = \langle\gamma_2\rangle = \langle\chi\rangle = 0$. In the case of HCN−$BF_3$, a value of $\gamma_{eff} \equiv \cos^{-1}[\langle\cos^2\gamma\rangle^{1/2}] = 17.5 \pm 0.2°$ was estimated from the nitrogen quadrupole coupling constant and $\chi_{eff} \equiv \cos^{-1}[\langle\cos^2\chi\rangle^{1/2}] = 13.1 \pm 1.3°$ was obtained from the boron coupling constant.

Preliminary analysis of the observed rotational constants indicated a boron−nitrogen distance of approximately 2.3 Å, a value which is almost exactly halfway between the van der Waals distance of 2.9 Å observed in N_2−BF_3[31] and the 1.58 Å sum of covalent bond radii for boron and nitrogen.[32] On the other hand, this same analysis yielded an N···H distance *r* of about 2.2 Å, very close to the 2.230 Å value observed in $(HCN)_2$.[33] Thus, the outer HCN appears weakly bound to the inner HCN, but the boron−nitrogen bond lies somewhere between a van der Waals interaction and a fully formed dative bond. Correspondingly, for the purpose of determining the structure of the complex, the C−H and C−N bond distances in the outer HCN were constrained to their values in free HCN in all subsequent analysis (1.06317 and 1.15538 Å, respectively[34]). For the inner HCN, however, as well as for the B−F bond distance in the BF_3, the use of free-molecule parameters is somewhat less clearly justified. Thus, to asses the affect of this ambiguity on the fitted structure of the complex, two limiting cases were identified.

The first limiting case is a "van der Waals" structure, in which the C−H and C−N bond lengths of the inner HCN, as well as the B−F bond length of the BF_3 were all constrained to their free-molecule values ($r_{CH} = 1.06317$ and $r_{CN} = 1.15538$ Å,[34] as above, and $r_{BF} = 1.3102$ Å[35,36]). For this structure, the angular vibrational amplitude of the BF_3 was taken to be $\chi_{eff} = 13.1°$, as in HCN−BF_3. For γ_2, a Kraitchman analysis[37,38] of the hydrogen and nitrogen coordinates of the outer HCN gave 11-(2)°, where the relatively large uncertainty arises from that in the rotational constants of the deuterated species. For γ_1, on the other hand, a similar analysis could not be performed since the inner nitrogen lies virtually on top of the center of mass of the complex, as noted above. For this reason, a value equal to γ_2 (11°) was utilized as a conservative upper limit for γ_1, which is reasonable inasmuch as the B−N bond is likely stronger than the N···H hydrogen bond, and the inner HCN is constrained by binding partners on both sides. Because the effects of these constraints on the angular vibrational amplitude are unknown, however, a lower limit of $\gamma_1 = 0$ was also considered. The second limiting case involves a "fully bonded" structure, in which the B−F bond length and the internal bond lengths of the inner HCN were constrained to their values in crystalline HCN−BF_3[18] ($r_{CH} = 0.96$ Å, $r_{CN} = 1.122$ Å, and $r_{BF} = 1.361$ Å.[39] In this limit, since the HCN−BF_3 is considered fully bonded, only $\gamma_1 = 0$ and $\chi = 0$ need be considered. γ_2, however, was still constrained to 11° since HCN(2) remains weakly bonded to HCN(1).

TABLE 3: Average Structural Parameters Determined for the Ground Vibrational State of HCN···HCN−BF_3

parameter	value
R(B−N)	2.299(28) Å
r(N···H)	2.185(25) Å
α(NBF)	93.5(3)°
γ_2[a]	11(2)°

[a] Determined from double-substitution Kraitchman analysis.

The preferred structural parameters for HCN···HCN−BF_3 were obtained from a series of nonlinear least-squares fits in which *R*, *r*, and α were varied (two for the "van der Waals" limiting structure, with $\gamma_1 = 0°$ and $\gamma_1 = 11°$, as discussed above) and one for the "fully bonded" limiting structure. Final values for *R*, *r*, and α were taken as the average between the highest and lowest values obtained, with an uncertainty chosen to encompass all values. The results are presented in Table 3. It should be noted that the values of *R* corresponding to the two choice for γ_1 (0° and 11°) are 2.272 and 2.289 Å, respectively, while the change to the fully bonded structure produces a bond distance of 2.326 Å. Thus, the choice of model contributes significantly to the uncertainty in the boron−nitrogen bond distance. The values of *r* and α, on the other hand are much less sensitive, as reflected in the error bars given for those numbers in the table. The structure is even less sensitive to the choice of χ_{eff}. For example, changing χ_{eff} from 13.1° to 0° in the weakly bound case changes *R* and *r* by less than 0.002 Å each. It is perhaps worth noting that the B−N bond energy is fairly low (4−7 kcal/mol, as described below), suggesting that the van der Waals limiting structure may be the more appropriate one to use. For this reason, the fully bonded model probably offers a very conservative limit as to the effect of modified monomer structural properties on the reported bond lengths in the complex.

Finally, it is reassuring to note that the fitted values of *R* and α are entirely consistent with the previously derived bond length−bond angle relationship[40] for adducts of BF_3 with nitrogen donors, viz.,

$$R(\mathrm{BN}) = (1.580\ \text{Å}) - (0.441\ \text{Å}) \log[9\cos^2\alpha] \qquad (2)$$

where the numerical parameters were derived from a least-squares fit to structural data for a variety of complexes. Using the fitted value of *R* in Table 3, eq 2 predicts a value of α equal to 92.9°, remarkably close to the quoted value of 93.5(3)°.

Discussion

Molecular Structure. The structural and spectroscopic properties of HCN···HCN−BF_3 provide information about the effect of a single near neighbor on the partial dative bond in HCN−BF_3. These effects are most easily evaluated in the context of comparisons with related systems, and a number of the relevant properties are summarized in Table 4.

The most striking feature of HCN···HCN−BF_3 is the 0.174(57) Å reduction of the B−N bond length relative to that in the isolated HCN−BF_3 adduct. To put this observation in perspective, we note that gas-to-solid structure changes for most covalently bonded molecules involve bond length changes of only a few thousandths to a few hundredths of an angstrom.[43,44] Moreover, such changes arise, in principle, from the cumulative

TABLE 4: Structural and Electronic Properties for HCN···HCN−BF_3 and Related Complexes

HCN(1)-BF_3[a]	HCN(2)···HCN(1)−BF_3[b]	HCN(2)···HCN(1)−SO_3[c]
R(N(1)−B) = 2.473(29) Å	R(N(1)−B) = 2.299(28) Å	R(N(1)−S) = 2.470(20) Å
α(NBF) = 91.5(1.5)°	α(NBF) = 93.5(3)°	α(NSO) = 92.2(6)°
γ_1 = 17.53(16)°	r(N(2)···H) = 2.185(25) Å	r(N(2)···H) = 2.213(29) Å
	γ_2 = 11(2)°	γ_2 = 9.4°
eQq(N(1)) = −4.080(13) MHz	eQq(N(1)) = −3.994(22) MHz	eQq(N(1)) = -3.882(15) MHz
	eQq(N(2)) = −3.984(33) MHz	eQq(N(2)) = −4.053(15) MHz
eQq(^{11}B) = 2.731(36) MHz	eQq(^{11}B) = 2.509(20) MHz	

HCN(1)···HCN(2)	HCN(1)···HCN(2)···HCN(3)[f]
r(N(1)···H) = 2.230 Å[d]	r(N(1)···H) = 2.17 Å
	r(N(2)···H) = 2.18 Å
γ_1 = 13.7°[e]	γ_1 = 12.6°
γ_2 = 9.0°[e]	γ_2 = 6°[g]
	γ_3 = 8.6°
eQq(N(1)) = −4.097(20) MHz[d]	eQq(N(1)) = −4.049(2) MHz
eQq(N(2)) = −4.440(19) MHz[d]	eQq(N(2)) = −4.251(2) MHz
	eQq(N(3)) = −4.375(1) MHz

[a] Reference 17. [b] This work. [c] Reference 14. [d] Reference 33. [e] Reference 41. [f] Reference 42. [g] Assumed value of ref 42.

effect of many interactions in the crystal. Thus, the 0.17 Å change in the HCN−BF_3 moiety resulting from a single near neighbor is extraordinary. Viewed in somewhat different terms, we observe that while the gas-phase bond length in HCN−BF_3 is 2.47 Å,[17] that in the solid is 1.64 Å,[18] a value which is very close to the sum of single bond covalent bond radii for boron and nitrogen (1.58 Å).[32] Thus, addition of a single remote HCN drives the dative bond about 20% of the way toward completion. The observed contraction is significantly larger than the 0.107(21) Å value previously reported for HCN···HCN−SO_3.[14]

Accompanying the crystallization of HCN−BF_3 is a large increase in the NBF bond angle α from ∼91.5° in the gas to 105.6° in the solid. Thus, a corresponding increase in this angle may also expected as microsolvation drives the dative bond formation forward. Such an increase in indeed suggested in Table 4, though the change is small and the uncertainties preclude a definitive assessment. A small change is not surprising, however, as the bond length−bond angle relationship expressed in eq 2 is rather flat in the vicinity of 2.5 Å, with an angular increase of only about 1° anticipated on the basis of the observed 0.17 Å contraction of the B−N bond.

It is also of interest to consider the nature of the HCN/HCN−BF_3 interaction in the immediate vicinity of contact, i.e., at the HCN···HCN hydrogen bond. Clearly, from the data in Table 4, while a significant shortening the B−N dative bond arises from microsolvation by HCN, the N···H hydrogen bond itself appears similar to that in $(HCN)_2$. The N···H distance in HCN···HCN−BF_3, for example, is only 0.045(25) Å shorter than that in $(HCN)_2$ and the angular vibrational amplitudes of the nitrogen-bound HCN (γ_1 in HCN(1)···HCN(2) and γ_2 in HCN(2)···HCN(1)−BF_3) differ only slightly outside the estimated uncertainty of our determination. These results are similar to those previously obtained for HCN···HCN−SO_3.[14] It is interesting to note that, some years ago, Gutowsky and co-workers reported a series of studies on complexes of the form HCN···HCN···Y (Y = CO_2, HCF_3, HF, and HCl),[45] in which all species displayed measurable changes in r(N···H) and r(N···Y) between the dimers and trimers. Values of these changes are listed in Table 5, together with those for the complexes for which Y = BF_3 and SO_3. It is apparent that that the observed reductions in r(N···H) for both HCN···HCN−BF_3 and HCN···HCN−SO_3 are commensurate with those observed in other weakly bound systems, while differences in the B−N and S−N bond lengths are much larger. We attribute this difference to the ability to form a new bond, either to BF_3 because of electron deficiency or SO_3 due to a propensity for octet expansion. The HCN···HCN interaction, on the other hand, cannot progress beyond a hydrogen bond, thus rendering it much less susceptible to external influence. Indeed, the results indicate that in both systems, the weak, closed-shell interactions remain weak, but that incipient bond formation is driven forward by the influence of a single "solvent" molecule.

TABLE 5: Bond Length Changes for Complexes with the General Formula HCN···HCN−Y

complex	ΔR(N−Y)[a] (Å)	Δr(N···H)[b] (Å)
HCN···HCN−BF_3[c]	0.174(57)	0.045(25)
HCN···HCN−SO_3[d]	0.107(21)	0.017(29)
HCN···HCN···CO_2[e]	0.052	0.004
HCN···HCN···HCF_3[e]	0.042	0.030
HCN···HCN···HF[e]	0.043	0.069
HCN···HCN···HCl[e]	0.062	0.054

[a] Distance in the dimer minus distance in the trimer. [b] Distance in $(HCN)_2$ minus distance in the trimer. [c] Dimer value of ref 17. Trimer value of this work. [d] Reference 14. [e] Reference 45.

The observed structure may also be examined in the context of previous theoretical studies on HCN−BF_3. In an early report, Jiao and Schleyer used the self-consistent reaction field (SCRF) method to predict large changes in structure and dipole moment for the adduct when placed in a polarizable, dielectric continuum.[9] Their results demonstrated that it is the interaction between the molecule and the Onsager reaction field which drives the system from its gas phase to its condensed phase structure. Moreover, the calculations indicated that at a dielectric constant of about 10, the field is sufficient to render the transformation complete. It is interesting to comment in this regard that addition of a single HCN unit onto the symmetry axis of HCN−BF_3 introduces an electric field along the same direction as the reaction field present in the SCRF calculation. Moreover, while the spatial variation of these two fields certainly differ, their effect, in terms of driving the dative interaction forward, is similar. In this spirit, direct comparison between the SCRF results and the experimental structure reported here, shows that the single HCN unit added to the adduct reduces the B−N bond length by an amount comparable to the reduction realized in a medium with a dielectric constant equal to 7.

From a cluster standpoint, the critical question is how many discrete near neighbors are required to realize the full transformation from gas phase to solid state structure. While, clearly, such an issue does not lend itself to continuum models, several workers have addressed the problem computationally for

$HCN-BF_3$ and $(HCN-BF_3)_2$, which together allow the influence of a single near neighbor to be assessed. Initially, Iglesias, Sordo, and Sordo[46] determined a side-by-side, antiparallel configuration for the dimer, and concluded that a single near neighbor could account for only a small fraction of the observed gas-to-solid structure changes. Later, however, using somewhat different basis sets, Cabaleiro-Lago and Ríos[12] reaffirmed the antiparallel configuration, but found that the first near neighbor indeed accounts for most of the observed structure change upon crystallization. While $HCN\cdots HCN-BF_3$ certainly differs from the $(HCN-BF_3)_2$ in that the near neighbor is along the C_3 axis of the $HCN-BF_3$ moiety (rather than alongside and antiparallel to it), the experimental results clearly demonstrate that a single binding partner can, indeed, account for a large fraction of the total bond contraction. What this means quantitatively in terms of the effect of a single $HCN-BF_3$ on its neighbor in the crystal is, of course, unclear, but the observation of a large change in response to a single HCN microsolvent indicates that substantial effect is entirely reasonable. Interestingly, Hankinson et al.[47] have shown that dipole−dipole interactions between adjacent molecules in the $HCN-BF_3$ crystal account for over one-third of the total molar lattice energy, consistent with the idea that a few nearest neighbor interactions are the most important.

Electronic Redistribution and Molecular Energetics. The observed nuclear quadrupole coupling constants in Table 4, are also consistent with an advancement of dative bond formation upon microsolvation, though the effects are generally much less pronounced. The value of eQq(^{11}B), for example, decreases from 2.731(36) MHz in $HCN-BF_3$ to 2.509(20) MHz in $HCN\cdots HCN-BF_3$. The former is essentially identical with that in weakly bound $Ar-BF_3$,[31] and has been interpreted as arising predominantly from the projective reduction due to large amplitude zero point vibration along the χ coordinate.[17] On the other hand, it seems unlikely that the further decrease in this value observed in $HCN\cdots HCN-BF_3$ could arise from vibrational effects alone, inasmuch as such a reduction would require an *increase* in bending amplitude from 13.1° in $HCN-BF_3$ to 19° in $HCN\cdots HCN-BF_3$. Such a value is too large, even for weakly bound BF_3, and the change, moreover, is in a direction that would be counterintuitive in view of the increased binding suggested by other structural and spectroscopic parameters. Similarly, the reduction in magnitude of eQq(N(1)) in $HCN(2)\cdots HCN(1)-BF_3$ (−3.994(22) MHz) relative to that in $HCN-BF_3$ (−4.080(13) MHz) is in the direction opposing that expected for a decreased vibrational amplitude, and a direct effect due to the field from the neighboring HCN unit seems unlikely in light of the quadrupole coupling constants in $(HCN)_2$ and $(HCN)_3$. Thus, while eQq(N(1)) is obviously not a very sensitive indicator, the small discernible changes in its magnitude also hint at electronic rearrangement near the dative bond site.

Additional information about the system is provided by the BLW-ED results given in Table 2. The binding energy of $HCN-BF_3$ of only 4.1 kcal/mol is somewhat below other estimates in the literature, which range from about 4.4−7.2 kcal/mol.[9,11,47,48] The disparity probably arises from the use of smaller basis sets, which are necessary to implement the BLW-ED scheme. Nevertheless, as we have argued previously for this complex,[17] the B−N dative bond is in an early stage of its formation, both from the standpoints of molecular structure and energetics. The calculated binding energy of 32.9 kcal/mol[11] for $(CH_3)_3N-BF_3$, in which the dative bond is fully formed, provides a useful reference point.

It is also apparent from Table 2 that the most significant energetic differences between $HCN-BF_3$ and $HCN\cdots HCN-BF_3$ arise from the distortion, polarization, and charge transfer energies. As expected, each of these terms contributes more in the latter complex. Charge transfer accounts for nearly an additional 1 kcal/mol of stability in $HCN\cdot\cdot HCN-BF_3$, though its effect is somewhat mitigated by other contributions such as the distortion energy, which is 1.4 kcal/mol more positive. The net result of all contributions is that energy of $HCN\cdots HCN-BF_3$ relative to $(HCN)_2 + BF_3$ is 0.8 kcal/mol greater than that of $HCN-BF_3$ relative to $HCN + BF_3$. Stated differently, the effect of the remote HCN on the complex is to increase the effective dative bond energy by about 20%.[49] As in the case of $HCN\cdots HCN-SO_3$,[14] the polarization contribution to the increase in dipole moment is 6−7 times greater than the charge-transfer component for both species.

The EDD maps have a similar appearance for both the $HCN-BF_3$ and $HCN\cdots HCN-BF_3$. In both cases, polarization increases electron density on the nitrogen and the fluorines, while electron flow away from the nitrogen and toward the boron is seen to arise from charge transfer. Although quantitative differences in the degree of electron flow between the two systems are difficult to ascertain from the diagrams, the EDD maps, together with the structural and computational results above provide a clear picture of the effect of microsolvation of $HCN-BF_3$ by an additional HCN: The large magnitude of the bond contraction (0.174(57) Å), the increase in bond strength (20%), and the migration of charge from the HCN to the BF_3 indicate that the additional HCN unit drives the B−N dative bond forward measurably. It is reassuring that the maps in Figure 2c,d show very little change in the hydrogen bonding region, consistent with both the above conclusion that the $HCN\cdots HCN$ hydrogen bond is virtually identical to that in $(HCN)_2$, and with the picture previously described for $HCN\cdots HCN-SO_3$.

Conclusions

The structure of $HCN\cdots HCN-BF_3$ has been determined using microwave spectroscopy. The goal of this study was to quantitatively characterize the extent to which a single near-neighbor interaction promotes bond formation in a partially bound complex. We observe a 0.174(57) Å contraction of the N−B distance when a single HCN molecule is added to $HCN-BF_3$, indicating that one near neighbor is enough to induce a significant advancement of the dative bond. Ab initio energy decomposition analysis, electron density maps, and to some extent experimental quadrupole coupling constants, support this interpretation of the structural data. In contrast, the N···H hydrogen bond in $HCN\cdots HCN-BF_3$ remains much less perturbed compared with that in $(HCN)_2$. Thus, as in our previous study of $HCN\cdots HCN-SO_3$,[14] weak, closed-shell interactions remain weak, but incipient donor−acceptor bonding is driven forward by the interaction of the adduct with a nearby molecule. This result is consistent with the general observation that partially bound systems undergo large changes in response to a local environment[7,8,14] and represents a quantitative observation of the onset of the effect at the small cluster level.

We believe that the broader significance of this work is as follows: With much current interest in the role of solvation in chemical processes, systems which respond strongly to their environment are potentially attractive candidates for the quantification of microsolvation effects. In general, the large gas-to-solid structure changes which are characteristic of partially bound species suggest that such systems could be useful in this regard. The results of this study, as well as of our previous

investigation of HCN···HCN−SO_3, demonstrate that partially bound electron pair donor−acceptor complexes indeed offer the prospect of providing large and thus readily measurable effects even in very small clusters. The "solute−solvent" interactions, moreover, are ones which drive chemical change in the solute (i.e., promote the formation of a new bond), and this, perhaps, is an additional feature of interest. While rotational spectroscopy will certainly find its greatest value for small clusters, other spectroscopies (e.g., fluorescence, infrared, photoionization, etc.) may be able to provide information for larger systems closer to the limit of bulk phase solution. We suggest that partially bound molecules may present interesting experimental test systems, and an unusual and challenging case for solvation models, where the effects to be predicted are large and the separation between inter- and intramolecular interactions is not distinct.

Acknowledgment. This work is supported by the National Science Foundation, the donors of the Petroleum Research Fund, administered by the American Chemical Society, and the Minnesota Supercomputer Institute. We are also grateful to Dr. Yirong Mo for his assistance with the BLW-ED calculations.

Supporting Information Available: Tables of transition frequencies and residuals from the least-squares fits. This material is available free of charge via the Internet at http://pubs.acs.org.

References and Notes

(1) Cramer, C. J.; Truhlar, D. G. *Chem. Rev.* **1999**, *99*, 2161.

(2) Tapia, O.; Bertran, J., Eds. *Solvent Effects and Chemical Reactivity*; Kluwer: Dordrecht, 1996.

(3) Tomasi, J.; Persico, M. *Chem. Rev.* **1994**, *94*, 2027.

(4) For example, see: (a) Cossi, M.; Scalmani, G.; Rega, N.; Barone, V. *J. Chem. Phys.* **2002**, *117*, 43. (b) Cossi, M.; Barone, V. *J. Chem. Phys.* **2001**, *115*, 4708. (c) Li, J.; Zhu, T.; Cramer, C. J.; Truhlar, D. G. *J. Phys. Chem. A* **2000**, *104*, 2178. (d) Coutinho, K.; Canuto, S. *J. Chem. Phys.* **2000**, *113*, 9132. (e) Naka, K.; Sato, H.; Morita, A. Hirata, F.; Kato, S. *Theor. Chem. Acc.* **1999**, *102*, 165. (f) Hawkins, G. D.; Cramer, C. J. Truhlar, D. G. *J. Phys. Chem. B* **1998**, *102*, 3257. (g) Hall, N. E.; Smith, B. J. *J. Phys. Chem. A* **1998**, *102*, 3985. (h) Gao, J.; Alhambra, C. *J. Am. Chem. Soc.* **1997**, *119*, 2962. (i) Zeng, J.; Woywod, C.; Hush, N. S.; Reimers, J. R. *J. Am. Chem. Soc.* **1995**, *117*, 8618 and references therein.

(5) Also see: (a) Levy, R. M.; Gallicchio, E. *Annu. Rev. Phys. Chem.* **1998**, *49*, 531. (b) Improta, R.; Scalmani, G.; Barone, V. *Chem. Phys. Lett.* **2001**, *336*, 349. (c) Gregoire, G.; Brenner, V.; Millie, P. *J. Phys. Chem. A* **2000**, *104*, 5204. (d) Aida, M.; Yamataka, H.; Dupuis, M. *Theor. Chem. Acc.* **1999**, *102*, 262 and references therein.

(6) For example, see: (a) Zhong, Q.; Castleman, A. W., Jr. *Chem. Rev.* **2000**, *100*, 4039. (b) Brutschy, B. *Chem. Rev.* **2000**, *100*, 3891. (c) Dedonger-Lardeux, C.; Gregoire, G.; Jouvet, C.; Martrenchard, S.; Solgadi, D. *Chem. Rev.* **2000**, *100*, 4023. (d) Dessent, C. E. H.; Kim. J.; Johnson, M. A. *Acc. Chem. Res.* **1998**, *31*, 527. (e) Duncan, M. A. *Annu. Rev. Phys. Chem.* **1997**, *48*, 69. (f) Lisy, J. M. *Int. Rev. Phys. Chem.* **1997**, *16*, 267. (g) Zwier, T. S. *Annu. Rev. Phys. Chem.* **1996**, *47*, 205. (h) Bernstein, E. R. Ed. *Chemical Reactions in Clusters*; Oxford: New York, 1996 and references therein.

(7) Leopold, K. R.; Canagaratna, M.; Phillips, J. A. *Acc. Chem. Res.* **1997**, *30*, 57.

(8) Leopold, K. R. In *Advances in Molecular Structure Research*; Hargittai, M. H., I., Ed.; JAI Press: Greenwich, CT, 1996; Vol. 2, p 103.

(9) Jiao, H.; Schleyer, P. v. R. *J. Am. Chem. Soc.* **1994**, *116*, 7429.

(10) Wong, M. W.; Wiberg, K. B.; Frisch, M. J. *J. Am. Chem. Soc.* **1992**, *114*, 523.

(11) Jonas, V.; Frenking, G.; Reetz, M. T. *J. Am. Chem. Soc.* **1994**, *116*, 8741.

(12) Cabaleiro-Lago, E. M.; Ríos, M. A. *Chem. Phys. Lett.* **1998**, *294*, 272.

(13) Hunt, S. W. Ph.D. Thesis, University of Minnesota, 2002.

(14) Fiacco, D. L.; Hunt, S. W.; Leopold, K. R. *J. Phys. Chem. A* **2000**, *104*, 8323.

(15) Michurin, A. A.; Krasnov, V. L.; Bodrikov, I. V. *J. Org. Chem. USSR* **1975**, *11*, 2512.

(16) Booth, H. S.; Martin, D. R. *Boron Trifluoride and Its Derivatives*; John Wiley and Sons: New York, 1949.

(17) Reeve, S. W.; Burns, W. A.; Lovas, F. J.; Suenram, R. D.; Leopold, K. R. *J. Phys. Chem.* **1993**, *97*, 10630.

(18) Burns, W. A.; Leopold, K. R. *J. Am. Chem. Soc.* **1993**, *115*, 11622.

(19) Mo, Y.; Gao, J.; Peyerimhoff, S. D. *J. Chem. Phys.* **2000**, *112*, 5530.

(20) Balle, T. J.; Flygare, W. H. *Rev. Sci. Instrum.* **1981**, *52*, 33.

(21) Phillips, J. A.; Canagaratna, M.; Goodfriend, H.; Grushow, A.; Almlöf, J.; Leopold, K. R. *J. Am. Chem. Soc.* **1995**, *117*, 12549.

(22) Phillips, J. A., Ph.D. Thesis, University of Minnesota, 1996.

(23) Legon, A. C.; Wallwork, A. L.; Rego, C. A. *J. Chem. Phys.* **1990**, *92*, 6397.

(24) Gillies, C. W.; Gillies, J. Z.; Sueram, R. D.; Lovas, F. J.; Kraka, E.; Cremer, D. *J. Am. Chem. Soc.* **1991**, *113*, 2412.

(25) Emilsson, T.; Klots, T. D.; Ruoff, R. S.; Gutowsky, H. S. *J. Chem. Phys.* **1990**, *93*, 6971.

(26) Canagaratna, M.; Phillips, J. A.; Goodfriend, H.; Leopold, K. R. *J. Am. Chem. Soc.* **1996**, *118*, 5290.

(27) Townes, C. H.; Schawlow, A. *Microwave Spectroscopy*; Dover: New York, 1975.

(28) Picket, H. M. *J. Mol. Spectrosc.* **1991**, *148*, 371. (b) http://spec.jpl.nasa.gov/.

(29) Frisch, M. J.; Trucks, G. W.; Schlegel, H. B.; Scuseria, G. E.; Robb, M. A.; Cheeseman, J. R.; Zakrzewski, V. G.; J. A. Montgomery, J.; Stratmann, R. E.; Burant, J. C.; Dapprich, S.; Millam, J. M.; Daniels, A. D.; Kudin, K. N.; Strain, M. C.; Farkas, O.; Tomasi, J.; Barone, V.; Cossi, M.; Cammi, R.; Mennucci, B.; Pomelli, C.; Adamo, C.; Clifford, S.; Ochterski, J.; Petersson, G. A.; Ayala, P. Y.; Cui, Q.; Morokuma, K.; Malick, D. K.; Rabuck, A. D.; Raghavachari, K.; Foresman, J. B.; Cioslowski, J.; Ortiz, J. V.; Baboul, A. G.; Stefanov, B. B.; Liu, G.; Liashenko, A.; Piskorz, P.; Komaromi, I.; Gomperts, R.; Martin, R. L.; Fox, D. J.; Keith, T.; Al-Laham, M. A.; Peng, C. Y.; Nanayakkara, A.; Gonzalez, C.; Challacombe, M.; Gill, P. M. W.; Johnson, B. G.; Chen, W.; Wong, M. W.; Andres, J. L.; Head-Gordon, M.; Replogle, E. S.; Pople, J. A. *Gaussian 98*, revision A.9; Gaussian, Inc.: Pittsburgh, PA, 1998.

(30) Boys, S. F.; Bernardi, F. *Mol. Phys.* **1970**, *19*, 553.

(31) Janda, K. C.; Bernstein, L. S.; Steed, J. M.; Novick, S. E.; Klemperer, W. *J. Am. Chem. Soc.* **1978**, *100*, 8074.

(32) Dvorak, M. A.; Ford, R. S.; Sueram, R. D.; Lovas, F. J.; Leopold, K. R. *J. Am. Chem. Soc.* **1992**, *114*, 108.

(33) Buxton, L. W.; Campbell, E. J.; Flygare, W. H. *Chem. Phys.* **1981**, *56*, 399.

(34) Winnewisser, G.; Maki, A. G.; Johnson, D. R. *J. Mol. Spectrosc.* **1971**, *39*, 149.

(35) Brown, C. W.; Overend, J. *Can. J. Phys.* **1968**, *46*, 977.

(36) Yamamoto, S.; Nakanaga, T.; Takeo, H.; Matsumura, C.; Takami, M.; Kuchitsu, K. *Chem. Phys. Lett.* **1985**, *122*, 9.

(37) Kraitchman, J. *Am. J. Phys.* **1953**, *21*, 17.

(38) Gordy, W.; Cook, R. L. *Microwave Molecular Spectra*; Wiley: New York, 1970.

(39) This value represents the average of three crystallographically distinct B−F bond distances in the crystal.

(40) Burns, W. A.; Phillips, J. A.; Canagaratna, M.; Goodfriend, H.; Leopold, K. R. *J. Phys. Chem.* **1999**, *103*, 7445.

(41) Ruoff, R. S.; Emilsson, T.; Chuang, C.; Klots, T. D.; Gutowsky, H. S. *Chem. Phys. Lett.* **1987**, *138*, 553.

(42) Ruoff, R. S.; Emilsson, T.; Klots, T. D.; Chuang, C.; Gutowsky, H. S. *J. Chem. Phys.* **1988**, *89*, 138.

(43) Hargittai, M.; Hargittai, I. *Phys. Chem. Miner.* **1987**, *14*, 413.

(44) Hargittai, I.; Hargittai, M. In *Molecular Structure and Energetics*; Liebman, J. F., Greenberg, A., Eds.; VCH Publishers: Deerfield Beach, 1987; Vol. 2, p 1.

(45) Ruoff, R. S.; Emilsson, T.; Chuang, C.; Klots, T. D.; Gutowsky, H. S. *J. Chem. Phys.* **1989**, *90*, 4069.

(46) Iglesias, E.; Sordo, T. L.; Sordo, J. A. *Chem. Phys. Lett.* **1996**, *248*, 179.

(47) Hankinson, D. J.; Almlöf, J.; Leopold, K. R. *J. Phys. Chem.* **1996**, *100*, 6904.

(48) Nxumalo, L. M.; Andrzejak, M.; Ford, T. A. *J. Chem. Inf. Comput. Sci.* **1996**, *36*, 377.

(49) We define the dative bond energy in this context as the energy change associated with the reaction D + BF_3 → D−BF_3, when D is HCN or HCN···HCN.